Journal of Civil Engineering and Urban Planning (2024)
Clausius Scientific Press, Canada

DOI: 10.23977/jceup.2024.060403
ISSN 2616-3969 Vol. 6 Num. 4

Finite Element Analysis of Monopile Horizontal Deformation under Cyclic Load

Xiaojian Luo[1,a], Changwei Shi[1,b], Songke Wei[1,c], Liangwei Sun[2,d], Chao Liang[2,e], Rui Liang[2,f,*]

[1]CNPC Offshore Engineering Company Limited, Beijing, 102600, China
[2]State Key Laboratory of Hydraulic Engineering Intelligent Construction and Operation, Tianjin University, Tianjin, 300072, China
[a]luoxj.cpoe@cnpc.com.cn, [b]shicw.cpoe@cnpc.com.cn, [c]weisk.cpoe@cnpc.com.cn, [d]sunliangwei0922@tju.edu.cn, [e]leongeo@foxmail.com, [f]jarheadyang@sina.com
[*]Corresponding author

Keywords: Offshore wind power, Pile foundation, Multidirectional cyclic load, Horizontal bearing capacity, Cumulative deformation

Abstract: Offshore wind power pile foundation will bear the horizontal static and dynamic loads generated by wind, wave and current during service, and its long-term stability has attracted much attention. Using numerical simulation as the analysis method and based on the stiffness attenuation model, a study was conducted on the cumulative deformation of a monopile under cyclic loading in sand, revealing the influence of the number of cyclic loads, amplitude, and soil parameters on the cumulative deformation of monopile. The results show that: the cumulative deformation of monopile is greatly affected by the amplitude of cyclic load. When $\zeta b < 0.4$, the cumulative deformation increases with the increase of the number of cyclic load and gradually tends to be stable; when ζb reaches 0.4, the cumulative deformation increases sharply with the increase of the number of cycles. The cumulative deformation of monopile increases gradually with the decrease of soil elastic modulus and friction angle. When the depth of monopile increases to a certain range, the sensitivity of cumulative deformation to soil elastic modulus decreases.

1. Introduction

Wind power has become a core sector in the development of renewable energy. Compared to onshore wind energy, offshore wind energy has a significant development potential due to its higher wind speeds, greater energy output, absence of noise pollution, and less land constraints. By the end of 2023, the global installed capacity of offshore wind power had reached 75.2 gigawatts (GW), marking a 24% increase from 2022. China surpassed the United Kingdom in 2021 to become the country with the largest cumulative installed capacity of offshore wind power globally and maintained this position in 2022 and 2023. Among existing offshore wind turbines, the monopile foundation (Figure 1) is the most widely used foundation type in offshore wind power. In recent years, as the unit capacity of individual turbines has gradually increased, the diameter of wind turbine piles has also expanded, with the largest monopile foundation diameters reaching up to 10 meters. During operation, wind turbines face complex load effects caused by wind, waves, and

currents in the marine environment, which pose threats to the safe operation of offshore wind turbines [1].

Figure 1: Monopile Foundation Structure

The analysis of existing monopile foundations under horizontal and bending moment loads generally adopts the *p-y* curve method recommended by the API[2] specification. This method is based on the test results of Matlock et al.[3] in 1970 and Reese et al.[4] in 1975, who conducted a small number of cyclic load tests on small-diameter flexible long piles. However, with the increase in the diameter of monopile foundations for existing wind turbines, the traditional *p-y* curve method can no longer meet the analysis of the load-bearing characteristics of large-diameter monopiles under horizontal and bending moment loads. In addition, regarding the impact of cyclic loading, the API specification only considers adding a correction factor based on the static load *p-y* curve, without taking into account the influence of the number of cyclic loads and the amplitude of cyclic loads on the horizontal bearing characteristics of the monopile. Long and Vanneste[5]'s cyclic loading test results in sandy soil show that the traditional *p-y* curve cannot accurately predict the development law of cumulative deformation of large-diameter monopiles under cyclic loading. In response to this issue, many scholars have conducted related research through centrifuge and numerical simulation. Peng et al.[6] developed a new type of eccentric wheel cyclic loading device to study the impact of cyclic loads on the horizontal bearing capacity of wing piles. Truong et al.[7] revealed the influence law of cyclic loads on the horizontal bearing capacity within the small cumulative deformation range of monopiles based on centrifuge tests. Guo Yushu et al.[8] developed a stiffness degradation model for sandy soil to analyze the cumulative deformation of monopiles using ABAQUS. Cao Guangwei et al.[9] studied the cumulative deformation, stiffness degradation, and pore pressure accumulation laws of large-diameter monopiles under different pile diameters and cyclic amplitude ratios based on centrifuge model tests of cyclic loading. Rudolph et al.[10] focused on the impact of the direction of cyclic loading on the cumulative deformation of monopiles in the centrifuge.

From the above research, it can be seen that the impact of cyclic loading on the bearing capacity and cumulative deformation of large-diameter monopiles in sandy soil is not negligible, but the existing research results have not yet reached a unified conclusion, and there is also a lack of effective and unified calculation methods. In particular, there is a lack of research on the dynamic response of monopiles under multi-directional cyclic loading. Therefore, this paper focuses on the issue of cumulative deformation of large-diameter monopiles under cyclic loading in sandy soil, using numerical simulation as a research tool, to carry out an analysis of the bearing performance of large-diameter monopiles in sandy soil, reveal the evolution law of cumulative deformation of monopiles, clarify the key factors affecting their bearing performance, and provide theoretical support for the safe operation of large-diameter monopiles in offshore wind power.

2. Numerical Analysis Model for Cumulative Deformation of Monopile

Conducting a study on the cumulative deformation of monopiles in sandy soil using numerical

analysis methods to reveal the influence patterns of various factors on the cyclic cumulative deformation of monopiles and to identify the key influencing factors.

2.1. Stiffness Degradation Model

The calculation employs ABAQUS as the numerical analysis software, and a stiffness degradation model program for sandy soil was written using USDFLD, as shown in the sandy soil stiffness degradation model [11], as depicted in Equation (1).

$$\delta = \frac{E_{sN}}{E_{s1}} = \frac{\varepsilon_{a1}}{\varepsilon_{aN}} = N^{-a(X_c)^b} \tag{1}$$

In the equation: ε_{a1} represents the axial plastic strain value under the first cycle of loading; ε_{aN} represents the axial plastic strain value under the Nth cycle of loading; a and b are stress parameters that can be determined through dynamic triaxial tests under different confining pressures; X_c is the characteristic cyclic stress ratio:

$$X_c = \frac{X^{(1)} - X^{(0)}}{1 - X^{(0)}} \tag{2}$$

$$X = \frac{\sigma_{cyc}}{\sigma_{sf}} \tag{3}$$

In the equation: X represents the cyclic stress ratio, $X^{(0)}$ denotes the cyclic stress ratio in the pile-soil system in the initial state; $X^{(1)}$ denotes the cyclic stress ratio in the pile-soil system after the application of horizontal cyclic loading; σ_{cyc} is the maximum principal stress during the cyclic loading process; σ_{sf} is the principal stress experienced by the soil at the time of static failure, which is related to the internal friction angle of the sandy soil and the minimum principal stress σ_3, as shown in Equation (5):

$$\sigma_{sf} = \frac{(1+\sin\varphi)\ \sigma_3 + 2c\cos\varphi}{1-\sin\varphi} \tag{4}$$

Referring to the suggestions of Kuo et al. [12], the stiffness degradation coefficients for medium-dense sand and dense sand are shown in Equations (6) and (7), respectively.

medium density sand: $$\delta = \frac{E_{sN}}{E_{s1}} = \frac{\varepsilon_1^a}{\varepsilon_N^a} = N^{-0.16(X_C)^{0.38}} \tag{5}$$

mercuric sulfide: $$\delta = \frac{E_{sN}}{E_{s1}} = \frac{\varepsilon_1^a}{\varepsilon_N^a} = N^{-0.2(X_C)^{5.76}} \tag{6}$$

2.2. Validation of the Stiffness Degradation Model

To verify the reliability of the stiffness degradation model in calculating the long-term cumulative deformation of monopile foundations, a three-dimensional finite element numerical model was established based on the centrifuge model tests of monopile foundations conducted by Truong et al. [7] in sandy soil with relative densities of 51% and 85%. To enhance computational efficiency, a 1/2 symmetric model was used, with both the pile and soil modeled using solid elements. The pile was modeled using a linear elastic model, and the soil was modeled using the Mohr-Coulomb elastoplastic model, with all grid cell types being C3D8. The radial dimension of the soil was 24*D*, and the longitudinal dimension was *L*+5*D*. The grid was sown with single

precision, densely arranged around the pile model, as shown in Figure 2.

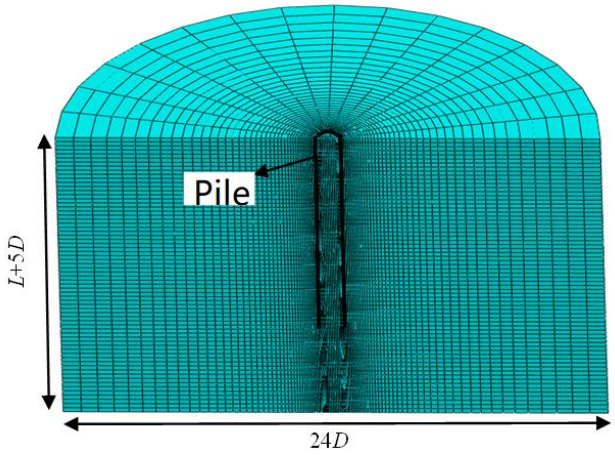

Figure 2: Numerical Calculation Model

The comparison of calculation results with the centrifuge test results is shown in Figure 3.

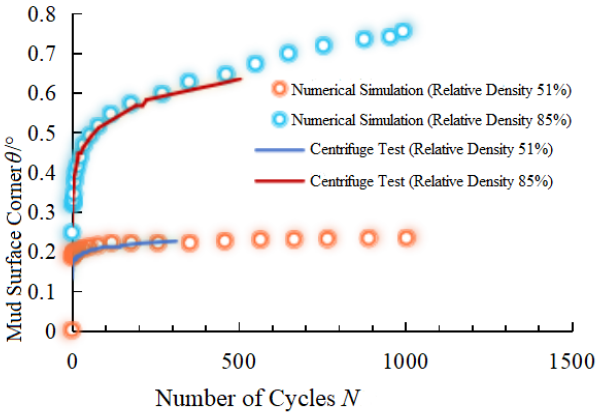

Figure 3: Comparison of Finite Element Calculation Results with Centrifuge Test Results

As can be seen from Figure 3, the development trend of the cumulative rotation angle calculated by the numerical simulation is basically consistent with the measured results of the centrifuge test, which can accurately predict the development law of the cumulative deformation of the pile body. The comparison between the numerical results and the centrifuge model test results validates the reliability of the stiffness degradation model used in the calculation.

3. Analysis of Cumulative Deformation Influencing Factors

3.1. Validation of the Stiffness Degradation Model

In order to study the impact of different pile diameters on cumulative deformation, three-dimensional finite element pile-soil models with pile diameters ranging from 5m to 8m were established. A horizontal cyclic load with an amplitude of 3MN was applied at the pile-soil interface, with a pile penetration depth of 30m. The calculation results are shown in Figure 4.

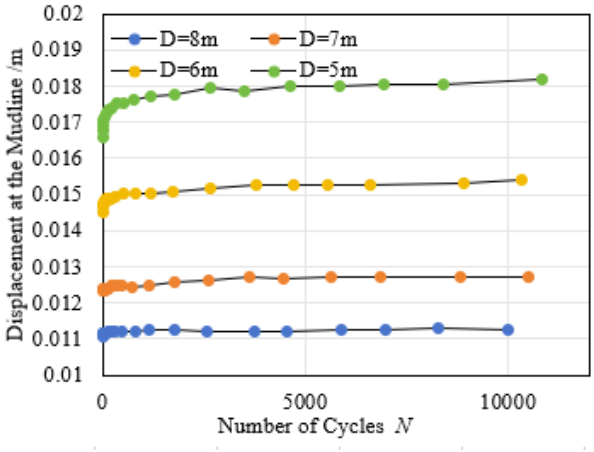

Figure 4: The Impact of Different Pile Diameters on Cumulative Deformation

As can be seen from Figure 4, when the pile diameters are 5m, 6m, 7m, and 8m, respectively, the horizontal displacement after 10,000 cycles of loading has increased by 9.7%, 5.8%, 3.1%, and 1.7% compared to the horizontal displacement after the first cycle of loading. With the increase in pile diameter, the displacement at the top of the pile after 10,000 cycles of loading is significantly reduced. Increasing the diameter of the pile can effectively reduce the cumulative deformation of the monopile foundation under cyclic loading.

3.2. The Impact of Pile Embedment Depth

By establishing pile-soil models with different embedment depths to study the impact of embedment depth on cumulative deformation, pile foundations with embedment depths of 20m, 30m, 40m, and 50m were created in the finite element software. The relationship between the displacement at the top of the pile and the number of cycles of horizontal cyclic loading of 3MN was investigated. The calculation results are shown in Figure 5.

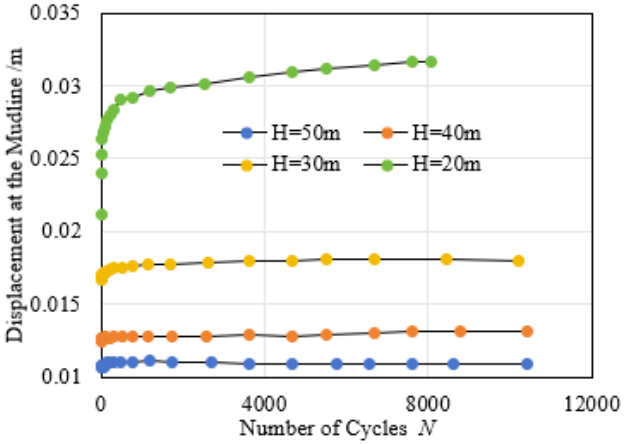

Figure 5: The Impact of Different Embedment Depths on Cumulative Deformation

As can be seen from Figure 5, the cumulative deformation of the monopile foundation significantly decreases with the increase in the embedment depth of the pile. When the number of cyclic loadings reaches 10,000, the cumulative deformation of the foundation with an embedment depth of 50 meters is nearly 67% less than that of the foundation with an embedment depth of 20 meters. When the pile diameter is 5 meters and the embedment depth exceeds 40 meters, further increasing the embedment depth results in a reduction of cumulative deformation of no more than

5%.

3.3. The Impact of Cyclic Load Amplitude

In order to study the impact of cyclic load amplitude on cumulative deformation, a model pile with a diameter of 5 meters and an embedment depth of 30 meters was established. Before conducting the cyclic load calculations, the pile was subjected to static loading to obtain the displacement-load curve at the mudline. The horizontal bearing capacity (Hult) of the model pile is approximately 40MN.

The equivalent parameter ζ_b of cyclic load represents the amplitude of cyclic loading as shown in Equation (7).

$$\zeta_b = H / H_{ult} \tag{7}$$

Subsequently, cyclic loads with amplitudes of ζ_b=0.2(H=8MN), 0.3(H=12MN), and 0.4(H=16MN) were applied to the model pile, respectively. When the number of cycles reached 10,000, the relationship between the cumulative deformation at the mudline and the number of cycles is shown in Figure 6.

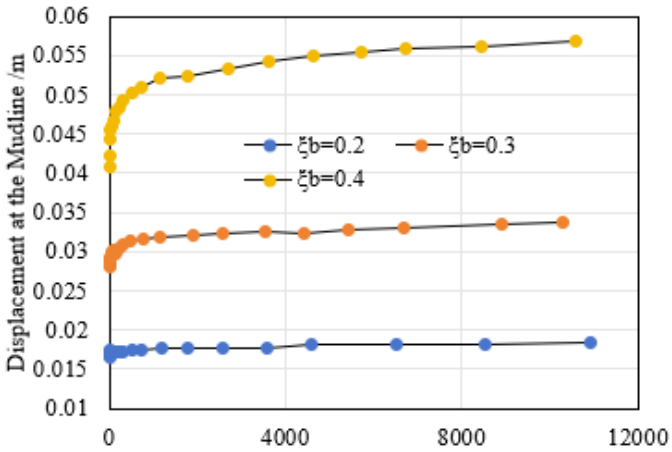

Figure 6: The Impact of Different Cyclic Load Amplitudes on Horizontal Displacement at the Top of the Pile

When the cyclic load amplitude ζ_b is between 0.2 and 0.3, the horizontal displacement at the top of the pile gradually tends to stabilize with the increase in the number of cyclic load applications. However, when the cyclic load amplitude increases to ζ_b=0.4, significant cumulative deformation occurs in the pile body under the action of cyclic loading. After 10,000 cycles, the increase in horizontal displacement at the mudline is as high as 40%. This indicates that as the amplitude of the cyclic load increases, the cumulative deformation also shows an increasing trend.

3.4. The Impact of Sandy Soil Parameters

(1) Soil Elastic Modulus

Models of pile-soil interaction were established with embedment depths of L=30m and 50m, and with sandy soil elastic moduli E of 10MPa, 30MPa, and 50MPa, respectively. A horizontal cyclic load with an amplitude of 3MN was applied, and the variation of horizontal displacement at the top of the pile with the number of cyclic load applications is shown in Figure 7.

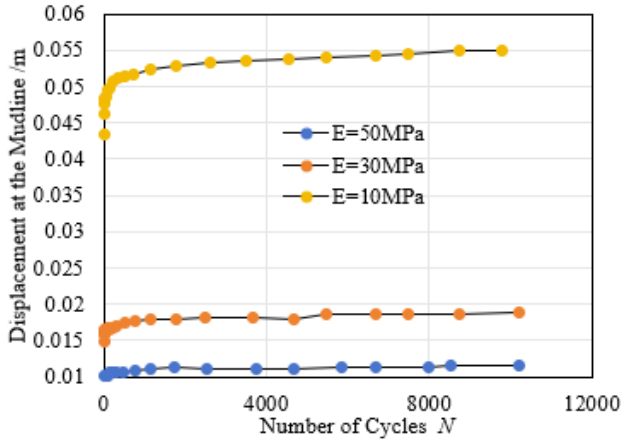

(a) L=30m

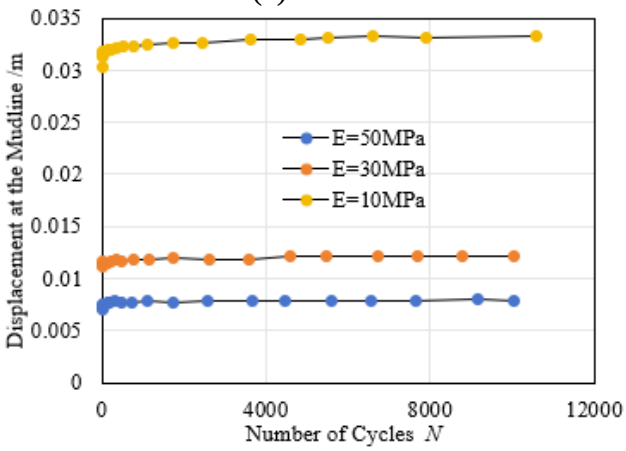

(b) L=50m

Figure 7: The Impact of Different Soil Elastic Moduli on Cumulative Deformation

According to the data shown in Figure 7, for the model pile with an embedment depth of 30 meters, after 10,000 cycles of loading, the horizontal displacement at the mudline increased by 26% and 22% when the soil elastic moduli were 10MPa and 30MPa, respectively. However, when the soil elastic modulus was raised to 50MPa, the displacement at the mudline essentially stopped increasing. Furthermore, as the embedment depth of the pile foundation increased to 50 meters, the sensitivity of cumulative deformation to soil elastic modulus significantly decreased. This indicates that an increase in the range of pile-soil interaction effectively suppresses the development of cumulative deformation caused by cyclic loading.

(2) Internal Friction Angle

The internal friction angle is a primary factor affecting the dynamic strength of sandy soil during cyclic shearing processes. Selecting the sand soil density according to $\phi'=16D_r^2+0.17D_r+28.4$, the internal friction angles of 34°, 38°, and 40° are taken in numerical calculations to simulate the foundations of medium-dense and dense sandy soils. Under the application of a horizontal cyclic load with an amplitude of 3MN, the impact of different internal friction angles on cumulative deformation is shown in Figure 8.

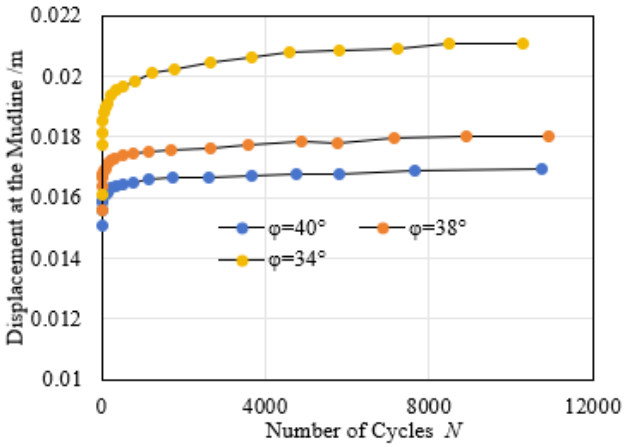

Figure 8: The Impact of Different Internal Friction Angles on Horizontal Displacement at the Top of the Pile

As can be seen from Figure 8, an increase in the internal friction angle significantly reduces the cyclic cumulative deformation of the monopile. When the internal friction angles are 34 °, 38 °, and 40 °, respectively, the horizontal displacement at the top of the pile after 10,000 cycles has increased by 32.1%, 15%, and 12.3% compared to the horizontal displacement at the top of the pile after the first cycle.

4. Conclusion

This paper analyzes the bearing characteristics of large-diameter monopile foundations for offshore wind power under cyclic loading through numerical simulation, revealing the development law of cumulative deformation of large-diameter monopiles in sandy soil. The specific conclusions are as follows:

(1) The stiffness degradation model can effectively simulate the cyclic cumulative deformation characteristics of monopile foundations. The development trend of the cumulative rotation angle calculated by numerical simulation is basically consistent with the measured results of the centrifuge test, which can accurately predict the development law of the pile body's cumulative deformation.

(2) Increasing the pile diameter and embedment depth can effectively reduce the horizontal displacement of monopile foundations under cyclic loading. When the amplitude of cyclic loading is small, the cumulative deformation gradually increases and tends to stabilize with the increase in the number of cyclic loadings; when the amplitude of cyclic loading increases to ζ_b=0.4, the cumulative deformation of the pile body will sharply increase with the increase in the number of cyclic loadings.

(3) The cumulative cyclic deformation of the monopile increases as the soil's elastic modulus decreases; as the embedment depth of the pile increases, the range of pile-soil interaction expands, and the cumulative deformation gradually decreases, with a threshold relative to the soil's elastic modulus, after which the sensitivity of cumulative deformation to the soil's elastic modulus decreases when the embedment depth reaches a certain range; the cumulative cyclic deformation of the monopile decreases as the internal friction angle of the soil increases.

References

[1] Wu Xiaoni, Liao Qian, Li Ye. A Review of the Load-Carrying Characteristics of Suction Bucket Foundations for Offshore Wind Turbines [J]. Journal of Ocean Technology, 2020, 39(01): 91-106.

[2] American Petroleum Institute (API). Geotechnical and Foundation Design Considerations[S]. Washington: API, 2011.
[3] Matlock H. Correlations for design of laterally loaded piles in soft clay[J]. Offshore Technology in Civil Engineering's Hall of Fame Papers from the Early Years, 1970, 1: 77-94
[4] Reese L C, Welch R C. Lateral loading of deep foundations in stiff clay[J]. Journal of the Geotechnical Engineering Division, 1975, 101(7): 633-649.
[5] Long J H, Vanneste G. Effects of cyclic lateral loads on piles in sand[J]. Journal of Geotechnical Engineering, 1994, 120(1): 225-244.
[6] Peng J, Clarke B G, Rouainia M. Increasing the resistance of piles subject to cyclic lateral loading[J]. Journal of Geotechnical and Geoenvironmental Engineering, 2011, 137(10): 977-982.
[7] Truong P, Lehane B M, Zania V, et al. Empirical approach based on centrifuge testing for cyclic deformations of laterally loaded piles in sand[J]. Géotechnique, 2019, 69(2): 133-145.
[8] Guo Yushu, Yakemus Martin, Abdurrahman Harri. Estimation of lateral deformation of monopile foundations by use of cyclic triaxial tests [J]. Chinese Journal of Geotechnical Engineering, 2009, 31(11): 1729-1734.
[9] Cao Guangwei, Ding Xuanming, Zhang Dingxin, et al. Bearing behaviors of large-diameter monopiles in soft clay under horizontal cyclic loading based on centrifugal model tests [J]. Chinese Journal of Geotechnical Engineering, 2023, 45(8): 1574-1585.
[10] Rudolph C, Bienen B, Grabe J. Effect of variation of the loading direction on the displacement accumulation of large-diameter piles under cyclic lateral loading in sand[J]. Canadian Geotechnical Journal, 2014, 51(10): 1196-1206.
[11] Achmus M, Kuo Y S, Abdel-Rahman K. Behavior of monopile foundations under cyclic lateral load[J]. Computers and Geotechnics, 2009, 36(5): 725-735.
[12] Kuo Y S, Achmus M, Abdel-Rahman K. Minimum embedded length of cyclic horizontally loaded monopiles[J]. Journal of Geotechnical and Geoenvironmental Engineering, 2012, 138(3): 357-363.